A Class of Halide-Supported Trinuclear Nickel Clusters [Ni 3 (μ 3 -L)(μ 3 -X)(μ 2 -dppm) 3] n + (L = I − , Br − , CO, CNR; X = I − , Br − ; n = 0, 1; dppm = Ph 2 PCH 2 PPh 2): No...

8 AUTHORS, INCLUDING:

Phillip E. Fanwick

Purdue University

640 PUBLICATIONS **11,121** CITATIONS

SEE PROFILE

Clifford P. Kubiak

University of California, San Diego

247 PUBLICATIONS **8,547** CITATIONS

SEE PROFILE

A Class of Halide-Supported Trinuclear Nickel Clusters [Ni$_3$(μ_3-L)(μ_3-X)(μ_2-dppm)$_3$]$^{n+}$ (L = I$^-$, Br$^-$, CO, CNR; X = I$^-$, Br$^-$; n = 0, 1; dppm = Ph$_2$PCH$_2$PPh$_2$): Novel Physical Properties and the Fermi Resonance of Symmetric μ_3-η^1 Bound Isocyanide Ligands

David A. Morgenstern,[‡] Gregory M. Ferrence, John Washington, Jason I. Henderson, Laurence Rosenhein,[§] Jerald D. Heise, Phillip E. Fanwick,[†] and Clifford P. Kubiak*

Contribution from the Department of Chemistry, Purdue University, 1393 Brown Laboratory, West Lafayette, Indiana 47907

Received August 31, 1995[⊗]

Abstract: The dihalide capped trinuclear nickel clusters Ni$_3$(μ_3-X)$_2$(μ_2-dppm)$_3$ (X = I (**1a**), Br (**1b**); dppm = Ph$_2$-PCH$_2$PPh$_2$) were synthesized and converted to their respective monocations [Ni$_3$(μ_3-X)$_2$(μ_2-dppm)$_3$]$^+$ (X = I (**1a**$^+$), Br (**1b**$^+$)) *via* a single electron oxidation. Clusters **1a** and **1a**$^+$ were characterized by X-ray crystallography. Displacement of a triply-bridging iodide ligand in Ni$_3$(μ_3-I)$_2$(μ_2-dppm)$_3$ (**1a**) by π-acceptor ligands produces a class of 48-electron trinuclear nickel clusters of the general formula [Ni$_3$(μ_3-L)(μ_3-I)(μ_2-dppm)$_3$]$^+$ (L = CO (**2a**); CNR, R = CH$_3$ (**3a**), 2,6-(CH$_3$)$_2$C$_6$H$_3$ (**4a**), *i*-C$_3$H$_7$ (**5**), C$_6$H$_{11}$ (**6**), *t*-C$_4$H$_9$ (**7**), CH$_2$C$_6$H$_5$ (**8**), C$_6$H$_5$ (**9**), *p*-C$_6$H$_4$I (**10**), *p*-C$_6$H$_4$-Br (**11**), *p*-C$_6$H$_4$Cl (**12**), *p*-C$_6$H$_4$F (**13**), *p*-C$_6$H$_4$CH$_3$ (**14**), *p*-C$_6$H$_4$CF$_3$ (**15**), *p*-C$_6$H$_4$OCH$_3$ (**16**), and *p*-C$_6$H$_4$CN (**17**)). A similar but less extensive study was conducted with the dibromide capped cluster **1b**. The X-ray crystal structure of cluster **2a**, as the PF$_6^-$ salt, was also obtained. Clusters **2−17** possess strikingly similar spectroscopic and electrochemical properties. This is ascribed to the lack of interaction between the a_2 LUMO of clusters **2−17** and the molecular orbitals of the capping π-acceptor ligands. The unexpected appearance of *two* ν(C≡N) bands in the FT-IR spectra of clusters **3−17** was demonstrated to be the result of a Fermi resonance involving the ν(C≡N) fundamental and the first overtone of the ν(N−C(alkyl)) fundamental of the capping isocyanide. In addition, molecular orbital calculations on **1−17** provide insights into the differences in the physical properties and reactivities of clusters of this class capped by π-donor (**1**) or π-acceptor ligands (**2−17**).

Introduction

The chemistry of homodinuclear[1] and heterodinuclear[2,3] transition metal complexes bridged by bis(diphenylphosphino)-methane (dppm = Ph$_2$PCH$_2$PPh$_2$) has developed considerably over the past 15 years. More recently it has become evident that dppm can also stabilize trinuclear clusters containing nickel or copper group metals with these triangular clusters containing at least one triply-bridging ligand.[4−12] An extensive exploration

of this area has been made by Puddephatt and co-workers, who synthesized the open-faced clusters [M$_3$(μ_3-CO)(μ_2-dppm)$_3$]$^+$ (M = Pd, Pt)[4] and [Pt$_3$(μ_3-H)(μ_2-dppm)$_3$]$^+$.[5] In addition, they observed that a variety of triply-bridging units such as Hg,[6] halides,[4] and vinylidenes[7] could be incorporated into the structure. Our laboratory has reported the synthesis and structure of [Ni$_3$(μ_3-CNCH$_3$)(μ_3-I)(μ_2-dppm)$_3$]$^+$ and its precursor, [Ni$_3$(μ_3-CNCH$_3$)(μ_3-I)(μ_2-dppm)$_2$(CNCH$_3$)$_2$]$^+$.[8,9] These clusters contain the first structurally characterized examples of isocyanides bound in a symmetric μ_3-η^1 fashion. Related to this, Puddephatt[10] has reported the synthesis of [Ni$_3$(μ_3-CO)-(μ_3-Cl)(μ_2-dppm)$_3$]$^+$ while Maekawa has recently published the synthesis and structure of Ni$_3$(μ_2-dppm)$_3$(μ_3-C≡CPh)$_2$.[13] Similar clusters of the group IB metals such as [Ag$_3$(μ_3-Cl)(μ_2-dppm)$_3$]$^+$ and [Cu$_3$(μ_3-C≡CPh)$_2$(μ_2-dppm)$_3$]$^+$ have also been prepared.[11,12]

The triangular nickel clusters synthesized in our laboratory have applications as electrocatalysts for the reduction of carbon dioxide. We have reported that [Ni$_3$(μ_3-CNCH$_3$)(μ_3-I)(μ_2-dppm)$_3$]$^+$ is an electrocatalyst for the reduction of CO$_2$ to the disproportionation products CO and CO$_3^{2-}$.[14−16] In addition,

[‡] Current Address: Los Alamos National Laboratory, Chemical Science and Technology Division, Los Alamos, NM 87545.

[§] Department of Chemistry, Indiana State University, Terre Haute, IN 47334.

[†] Address correspondence pertaining to crystallographic studies to this author.

[⊗] Abstract published in *Advance ACS Abstracts,* February 15, 1996.

(1) Puddephatt, R. J. *Chem. Soc. Rev.* **1983,** *12,* 99.

(2) (a) McDonald, W. S.; Pringle, P. G.; Shaw, B. L. *J. Chem. Soc., Chem. Commun.* **1982,** 861. (b) McDonald, W. S.; Pringle, P. G.; Shaw, B. L. *J. Chem. Soc., Chem. Commun.* **1982,** 81.

(3) Wang, L.-S.; Cowie M. *Organometallics* **1995,** *14,* 2374.

(4) Manojlović-Muir, L.; Muir, K. W.; Lloyd, B. R.; Puddephatt, R. J. *J. Chem. Soc., Chem. Commun.* **1985,** 536.

(5) Lloyd, B. R.; Puddephatt, R. J. *J. Am. Chem. Soc.* **1985,** *107,* 7785.

(6) Schoettel, G.; Vittal, J. J.; Puddephatt, R. J. *J. Am. Chem. Soc.* **1990,** *112,* 6400.

(7) Rashidi, M.; Puddephatt, R. J. *J. Am. Chem. Soc.* **1986,** *108,* 7111.

(8) Ratliff, K. S.; Fanwick, P. E.; Kubiak, C. P. *Polyhedron* **1990,** *9,* 1487.

(9) Ratliff, K. S.; Broeker, G. K.; Fanwick, P. E.; Kubiak, C. P. *Angew. Chem., Int. Ed. Engl.* **1990,** *29,* 395.

(10) Manojlović-Muir, L.; Muir, K. W.; Mirza, H. A.; Puddephatt, R. J. *Organometallics* **1992,** *11,* 3440.

(11) Franzoni, D.; Pelizzi, G.; Predieri, G.; Tarasconi, P.; Vitali, F.; Pelizzi, C. *J. Chem. Soc., Dalton Trans.* **1989,** 247.

(12) Diez, J.; Gamasa, M. P.; Gimeno, J.; Aguirre, A.; Garcia-Granda, S. *Organometallics* **1991,** *10,* 380.

(13) Maekawa, M.; Munakata, M.; Kuroda-Sowa, T.; Hachiya, K. *Inorg. Chim. Acta* **1995,** *233,* 1.

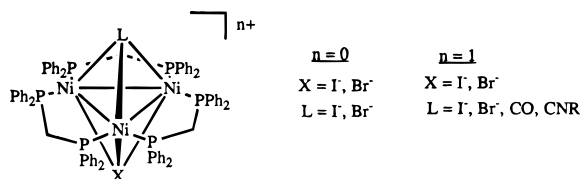(14) Ratliff, K. S. Ph.D. Thesis, Purdue University, 1990.

(15) Ratliff, K. S.; Lentz, R. E.; Kubiak, C. P. *Organometallics* **1992,** *11,* 1986.

Table 1. NMR and UV−Vis Data for [Ni$_3$(μ_3-L)(μ_3-X)(μ_2-dppm)$_3$]$^{n+}$ (n = 0, 1) Clusters

	X	L	^{31}P NMR^a	^{1}H NMR^a		UV−vis^b λ_{max}
				CH$_2$^{c}	Ph	
1a	I$^-$	I$^-$	−14.0	5.10	7.5−6.6	651.2 (7.8)^d
						514.0 (6.1)
1a$^+$	I$^-$	I$^-$	e	e	e	563.2 (12.6)
						434.0 (6.2)
1b	Br$^-$	Br$^-$	−11.5	4.28	7.4−6.6	672.0 (5.9)^d
						542.0 (7.9)
1b$^+$	Br$^-$	Br$^-$	e	e	e	554.0 (11.8)
						446.0 (6.0)
2a	I$^-$	CO	3.1	4.10	7.3−6.8	520.0 (6.3)
2b	Br$^-$	CO	2.3	3.99	7.7−6.8	516.0 (4.9)
3a	I$^-$	CNCH$_3$	0.4	4.05	7.3−6.8	527.0 (3.8)
3b	Br$^-$	CNCH$_3$	0.6	4.00	7.6−6.7	520.0 (3.2)
4a	I$^-$	CN(2,6-(CH$_3$)$_2$C$_6$H$_3$)	−1.9	4.10	7.2−6.7	542.2 (3.4)
4b	Br$^-$	CN(2,6-(CH$_3$)$_2$C$_6$H$_3$)	−2.5	4.28	7.4−6.8	534.0 (5.8)
5	I$^-$	CN(i-C$_3$H$_7$)	−0.2	4.10	7.3−6.8	534.4 (4.5)
6	I$^-$	CNC$_6$H$_{11}$	0.3	4.14	6.7−7.2	536.5 (5.0)
7	I$^-$	CN(t-C$_4$H$_9$)	−0.6	4.10	7.2−6.7	539.2 (3.8)
8	I$^-$	CNCH$_2$C$_6$H$_5$	0.4	4.11	7.3−6.8	529.3 (4.3)
9	I$^-$	CNC$_6$H$_5$	0.9	4.10	7.5−6.8	529.6 (3.6)
10	I$^-$	CN(p-C$_6$H$_4$I)	0.8	4.13	7.2−6.7	515.0 (4.0)
11	I$^-$	CN(p-C$_6$H$_4$Br)	1.2	4.08	7.3−6.8	528.4 (4.1)
12	I$^-$	CN(p-C$_6$H$_4$Cl)	1.2	4.08	7.5−6.7	544.0 (4.2)
13	I$^-$	CN(p-C$_6$H$_4$F)	−0.7	4.14	7.3−6.7	540.0 (4.1)
14	I$^-$	CN(p-C$_6$H$_4$CH$_3$)	0.8	4.10	7.1−6.8	531.2 (4.1)
15	I$^-$	CN(p-C$_6$H$_4$CF$_3$)	−1.0	4.16	7.1−6.7	526.0 (4.4)
16	I$^-$	CN(p-C$_6$H$_4$OCH$_3$)	0.7	4.09	7.2−6.8	529.6 (3.7)
17	I$^-$	CN(p-C$_6$H$_4$CN)	1.7	4.09	7.6−6.7	519.2 (4.8)

^{a} Chemical shifts given in ppm. **1a**, **1b** recorded in C$_6$D$_6$. **2a**, **3a**, **4a**, **5−8** recorded in CD$_3$CN. **1a$^+$**, **1b$^+$**, **2b**, **3b**, **9−17** recorded in CD$_2$Cl$_2$. **4b** recorded in C$_3$D$_6$O. ^{b} Recorded in CH$_3$CN; extinction coefficient ϵ (M^{-1}·cm^{-1} × 10^3) given in parentheses. ^{c} Chemical shift is assigned to the center of multiplet, dppm ligand protons only. ^{d} Recorded in toluene. ^{e} Paramagnetic.

Ni$_3$(μ_3-I)$_2$(μ_2-dppm)$_3$ has been used in the photochemical generation of the radical anion of carbon dioxide, CO$_2$$^{\bullet-}$, which can subsequently be used in the synthesis of organic dicarboxylic acids from olefins.[17] Thus, although some of the important reactions of this class of nickel clusters have been communicated, a full description of their synthesis and electronic structure and a systematic discussion of their novel physical properties have yet to be reported. Herein, we report the synthesis, structure, and electrochemistry of a family of clusters, [Ni$_3$(μ_3-L)(μ_3-X)(μ_2-dppm)$_3$]$^{n+}$. In addition, a theoretical study of the electronic structure of these clusters is described.

Experimental Section

Materials and Physical Measurements. All manipulations were performed under an N$_2$ atmosphere using an inert atmosphere glovebox or Schlenk techniques. Solvents were reagent or HPLC grade and dried over the appropriate drying agents. Anhydrous NiI$_2$ and isopropyl isocyanide were purchased from Strem and 2,6-dimethylphenyl isocyanide was purchased from Fluka. Dppm, *tert*-butyl isocyanide, cyclohexyl isocyanide, benzyl isocyanide, C$_6$H$_5$NH$_2$, p-IC$_6$H$_4$NH$_2$, p-BrC$_6$H$_4$NH$_2$, p-ClC$_6$H$_4$NH$_2$, p-FC$_6$H$_4$NH$_2$, p-CF$_3$C$_6$H$_4$-NH$_2$, p-CH$_3$C$_6$H$_4$-NH$_2$, p-CH$_3$OC$_6$H$_4$NH$_2$, p-NCC$_6$H$_5$NH$_2$, K^{13}CN, KC^{15}N, CH$_3$I, CD$_3$I, and ^{13}CH$_3$I were purchased from Aldrich; CO$_{(g)}$ was purchased from Matheson. All materials were used as received. Ni(COD)$_2$[18,19] and methyl isocyanide[20] were prepared by literature methods. Isotopically

labeled methyl isocyanides (CH$_3$N^{13}C, CH$_3$^{15}NC, ^{13}CH$_3$NC, CD$_3$NC) were prepared *via* the literature method using the appropriate combination of labeled potassium cyanide and methyl iodide.[21,22] The carbene method of isocyanide synthesis was used to prepare C$_6$H$_5$NC, C$_6$D$_5$-NC, p-IC$_6$H$_4$NC, p-BrC$_6$H$_4$NC, p-ClC$_6$H$_4$NC, p-FC$_6$H$_4$NC, p-CF$_3$C$_6$H$_4$-NC, p-CH$_3$C$_6$H$_4$NC, p-CH$_3$OC$_6$H$_4$NC, and p-NCC$_6$H$_4$NC.[23] ^{1}H and ^{31}P NMR spectra were obtained on Varian XL-200 or General Electric QE-300 spectrometers. ^{31}P chemical shifts were referenced with respect to external 85% H$_3$PO$_4$. All NMR spectra were obtained in CD$_3$CN or CD$_2$Cl$_2$ unless otherwise noted. Cyclic voltammetry was performed in acetonitrile containing 0.1 M tetrabutylammonium hexafluorophosphate (TBAP) using a Princeton Applied Research Model 173 potentiostat/galvanostat and Model 175 universal programmer. A gold working electrode, a platinum wire counter electrode, and a ferrocene/ferrocenium reference electrode were employed. Plasma desorption (PD) mass spectra were measured on an Applied Biosystems Bio-Ion 20R spectrometer. Calculated m/z for molecular ions are averages. UV−vis, ^{31}P NMR, and selected ^{1}H NMR data for **1−17** are summarized in Table 1; the FT-IR, MS, and electrochemical data are collected in Table 2.

Preparation of Ni$_3$(μ_3-I)$_2$(μ_2-dppm)$_3$ (1a). The preparation of complex **1a** has been described previously.[24] Anhydrous NiI$_2$ (0.57 g, 1.8 mmol) was dissolved in hot 2-methoxyethanol (150 mL). In a separate flask, Ni(COD)$_2$ (1.0 g, 3.6 mmol) was dissolved in 10 mL of toluene and 1.5 equiv of dppm (2.10 g, 5.5 mmol) was added, with stirring, to afford a red solution. This red intermediate was added to the NiI$_2$ solution leading to the immediate formation of **1a** as a green precipitate. The product was isolated by filtration and washed with

(16) Blaine, C.; Mann, K. R.; Wittrig, R. E.; Ferrence, G. M.; Washington, J.; Kubiak, C. P. *Organometallics* Submitted for publication.

(17) Morgenstern, D. A.; Wittrig, R. E.; Fanwick, P. E.; Kubiak, C. P. *J. Am. Chem. Soc.* **1993**, *115*, 6430.

(18) Schunn, R. A.; Ittel, S. D.; Cushing, M. A. In *Inorganic Syntheses*; Angelici, R. J., Ed; Wiley: New York: 1990; Vol. 28, pp 94−98.

(19) Guerrieri, F.; Salerno, G. *J. Organomet. Chem.* **1976**, *114*, 339.

(20) Casanova, J.; Schuster, R. E.; Werner, N. D. *J. Chem. Soc.* **1963**, 4280.

(21) Mottern, J. G.; Fletcher, W. H. *Spectrochim. Acta* **1962**, *18*, 995.

(22) DeLaet, D. L.; del Rosario, R.; Fanwick, P. E.; Kubiak, C. P. *J. Am. Chem. Soc.* **1987**, *109*, 754.

(23) Weber, W. P.; Gokel, G. W. *Tetrahedron Lett.* **1972**, *17*, 1637.

(24) Morgenstern, D. A.; Rothwell, A. P.; Bonham, C. C.; Wood, K. V.; Kubiak, C. P. *Polyhedron* **1995**, *14*, 1129.

Table 2. Infrared, Electrochemical, and Mass Spectral Data for [Ni$_3$(μ_3-L)(μ_3-X)(μ_2-dppm)$_3$]$^{n+}$ ($n = 0$, 1) Clusters

	X	L	FT-IR^a ν(C≡N)	$E_{1/2}$(+/0)^b (vs SCE)	mass spec.^{c} m/z
1a	I$^-$	I$^-$		< −2.0^d	1583 (1583)
1a$^+$	I$^-$	I$^-$		−0.68^d	1583 (1583)
1b	Br$^-$	Br$^-$		< −1.5	1491 (1489)
1b$^+$	Br$^-$	Br$^-$		−0.80	1488^e (1489)
2a	I$^-$	CO	1726^f	−1.12	1484 (1484)
2b	Br$^-$	CO	1724^f	−1.13	1437 (1437)
3a	I$^-$	CNCH$_3$	1927, 1872	−1.18	1497 (1497)
3b	Br$^-$	CNCH$_3$	1917, 1851	−1.26	1450 (1450)
4a	I$^-$	CN(2,6-(CH$_3$)$_2$C$_6$H$_3$)	1849, 1822	−1.08	1587^e (1586)
4b	Br$^-$	CN(2,6-(CH$_3$)$_2$C$_6$H$_3$)	1854, 1824	−1.16	1540 (1540)
5	I$^-$	CN(*i*-C$_3$H$_7$)	1876, 1815	−1.18	1525 (1526)
6	I$^-$	CN(*t*-C$_4$H$_9$)	1780 (broad)	−1.12	1539 (1540)
7	I$^-$	CNC$_6$H$_{11}$	1885, 1832	−1.17	1564 (1564)
8	I$^-$	CNCH$_2$C$_6$H$_5$	1887, 1801	−1.11	1573 (1572)
9	I$^-$	CNC$_6$H$_5$	1818, 1759	−1.06	1560 (1558)
10	I$^-$	CN(*p*-C$_6$H$_4$I)	1794, 1751	−1.00	1684 (1685)
11	I$^-$	CN(*p*-C$_6$H$_4$Br)	1812, 1758	−1.14	1639 (1638)
12	I$^-$	CN(*p*-C$_6$H$_4$Cl)	1811, 1756	−1.14	1594 (1594)
13	I$^-$	CN(*p*-C$_6$H$_4$F)	1805, 1757	−1.16	1577 (1577)
14	I$^-$	CN(*p*-C$_6$H$_4$CH$_3$)	1820, 1771	−1.18	1574 (1573)
15	I$^-$	CN(*p*-C$_6$H$_4$CF$_3$)	1800, 1731	−1.09	1628 (1629)
16	I$^-$	CN(*p*-C$_6$H$_4$OCH$_3$)	1804 (broad)	−1.19	1590 (1589)
17	I$^-$	CN(*p*-C$_6$H$_4$CN)	1782, 1718	−1.13	1584 (1584)

^{a} Recorded as KBr pellets, cm^{-1}. ^{b} Cyclic voltammograms recorded in CH$_3$CN. ^{c} Plasma desorption, 15 000 V, calculated mass in parentheses. ^{d} Recorded in 1,1,1-trichloroethane. ^{e} FAB. ^{f} ν(CO).

hexane to yield 2.5 g (87%) of **1a**. Anal. Calcd for C$_{75}$H$_{66}$I$_2$Ni$_3$P$_6$: C, 56.90; H, 4.20. Found: C, 57.02; H, 4.39.

Preparation of [Ni$_3$(μ_3-I)$_2$(μ_2-dppm)$_3$][PF$_6$] (1a$^+$). Cluster **1a** (0.21 g, 0.13 mmol) was dissolved in 200 mL of THF and 0.034 g (0.13 mmol, 1.0 equiv) of AgPF$_6$ was added, leading to an immediate color change from green to purple corresponding to the oxidation of **1a** to **1a$^+$**. Silver metal was removed by filtering the solution through Celite. The product can be isolated by the addition of pentane. Yield: 0.16 g (68%).

Preparation of Ni$_3$(μ_3-Br)$_2$(μ_2-dppm)$_3$ (1b). This compound was made by a procedure similar to that used for the diiodide cluster **1a**. Anhydrous NiBr$_2$ (0.40 g, 1.83 mmol) was dissolved in 60 mL of hot methoxyethanol to form a slightly cloudy solution which was filtered before use. A solution of Ni(COD)$_2$ (1.0 g, 3.64 mmol) and dppm (2.10 g, 5.47 mmol) in 10 mL of toluene was added to the NiBr$_2$ solution. A brown microcrystalline precipitate formed immediately. After cooling to −10 °C, the solution was filtered and the solid washed with methanol and hexanes and dried under vacuum. Yield: 1.89 g (68%). Anal. Calcd for C$_{75}$H$_{66}$P$_6$Ni$_3$Br$_2$: C, 60.48; H, 4.47. Found: C, 60.20; H, 4.65.

Preparation of [Ni$_3$(μ_3-Br)$_2$(μ_2-dppm)$_3$][BF$_4$] (1b$^+$). Cluster **1b$^+$** was prepared from **1b** following a method similar to that used for **1a$^+$**. From **1b** (0.50 g, 0.34 mmol) and AgBF$_4$ (0.065 g, 0.34 mmol), **1b$^+$** was obtained as a purple solid. Yield: 0.35 g (66%).

Preparation of [Ni$_3$(μ_3-CO)(μ_3-I)(μ_2-dppm)$_3$][I] (2a). Cluster **1a** (0.39 g, 0.25 mmol) was dissolved in 50 mL of CH$_2$Cl$_2$. An excess of CO gas was bubbled through the green solution for 3 min and the solution was stirred for 1 h until the color changed to purple. The solution was purged with N$_2$ and the product precipitated by addition of 150 mL of pentane, recovered by filtration, and dried under vacuum. Yield: 0.34 g (85%).

Preparation of [Ni$_3$(μ_3-CO)(μ_3-Br)(μ_2-dppm)$_3$][Br] (2b). Cluster **2b** was prepared using a modification of Puddephatt's procedure for the synthesis of [Ni$_3$(μ_3-CO)(μ_3-Cl)(μ_2-dppm)$_3$][Cl].[10] Ni$_2$(μ_2-dppm)$_2$-(μ-CO)Br$_2$[25,26] (0.20 g, 0.19 mmol) was refluxed in toluene for 24 h and then evacuated to dryness. The residue was extracted into CH$_2$-Cl$_2$ (40 mL) and the product was precipitated with pentane (150 mL). Yield 0.16 g (83%).

Preparation of [Ni$_3$(μ_3-CNCH$_3$)(μ_3-I)(μ_2-dppm)$_3$][I] (3a). The preparation of the methyl isocyanide derivative (**3a**) is representative of the synthetic procedure used for **3−17**. Cluster **1a** (0.54 g, 0.34

mmol) was dissolved in 50 mL of CH$_2$Cl$_2$ and 1 equiv of methyl isocyanide (18 μL) was added with stirring. The solution turned violet within 5 min. The solution was stirred for 2 h to ensure complete reaction after which time 150 mL of pentane was added to induce precipitation. Cluster **3a** was recrystallized using CH$_2$Cl$_2$/hexane. Yield: 0.40 g (71%). ^{1}H NMR (CD$_3$CN): δ 4.20 (s, 3H, C*H$_3$*NC). The PF$_6$$^-$ salt of **3a** can be obtained by stirring a CH$_3$CN solution of **3a** with a 10-fold excess of NaPF$_6$. After removal of the acetonitrile, cluster **3a** is extracted into CH$_2$Cl$_2$, filtered, and precipitated using hexane.

Preparation of Isotopically Labeled [Ni$_3$(μ_3-L)(μ_3-I)(μ_2-dppm)$_3$]-[I], L = ^{13}CNCH$_3$ (3a-^{13}C), C^{15}NCH$_3$ (3a-^{15}N), CN^{13}CH$_3$ (3a-^{13}CH$_3$), CNCD$_3$ (3a-CD$_3$). Preparation of the isotopically labeled isocyanide capped trimers was similar to that for **3a** with substitution of the appropriately labeled methyl isocyanide.

Preparation of [Ni$_3$(μ_3-CNCH$_3$)(μ_3-Br)(μ_2-dppm)$_3$][Br] (3b). Ni$_2$-(μ_2-dppm)$_2$(μ_2-CNCH$_3$)(CNCH$_3$)$_2$[22] (1.54 g, 1.53 mmol) was dissolved in 50 mL of THF and NiBr$_2$ (0.33 g, 1.52 mmol) in 25 mL of THF was added. The reaction mixture was allowed to stir for 1 h during which time a purple solid formed. This was filtered, rinsed with pentane, and vacuum dried to obtain 0.98 g (52%) of [Ni$_3$(μ_2-dppm)$_2$-(μ_3-CNCH$_3$)(μ_3-Br)(CNCH$_3$)$_2$][Br] (**18**). IR (KBr) ν(CN): 2167, 1951 cm^{-1}. ^{31}P NMR (CD$_3$CN) δ 1.92, 1.84 (AA′BB′). Subsequently, **18** (0.98, 0.79 mmol) was dissolved in 50 mL of CH$_3$CN to which dppm (0.40 g, 1.04 mmol) was added. The reaction was refluxed for 2 days and filtered, and the filtrate was dried under vacuum. The residue was extracted into 50 mL of CH$_2$Cl$_2$, precipitated with pentane (150 mL), and filtered to give **3b**. Yield: 0.89 g (74%). ^{1}H NMR (CD$_3$CN): δ 4.25 (s, 3H, C*H$_3$*NC). Cluster **3b** can also be prepared *via* addition of CNCH$_3$ to **1b**.

Preparation of [Ni$_3$(μ_3-CN(2,6-Me$_2$C$_6$H$_3$))(μ_3-I)(μ_2-dppm)$_3$][I] (4a). Following a method similar to the preparation of **3a**, **1a** (1.0 g, 0.63 mmol) and 2,6-dimethylphenyl isocyanide (0.083 g, 0.63 mmol) gave **4a**. Yield: 0.58 g (63%). ^{1}H NMR (CD$_3$CN): δ 2.11 (s, 6H, ((C*H$_3$*)$_2$C$_6$H$_3$)NC).

Preparation of [Ni$_3$(μ_3-CN(2,6-Me$_2$C$_6$H$_3$))(μ_3-Br)(μ_2-dppm)$_3$][Br] (4b). Following a method similar to the preparation of **3a**, **1b** (0.50 g, 0.34 mmol) and 2,6-dimethylphenyl isocyanide (0.043 g, 0.33 mmol) gave **4b**. Cluster **4b** was recrystallized from THF/hexane to give a red-brown solid. Yield: 0.21 g (40%). ^{1}H NMR (CD$_3$CN): δ 2.15 (s, 6H, ((C*H$_3$*)$_2$C$_6$H$_3$)NC).

Preparation of [Ni$_3$(μ_3-CN(*i*-C$_3$H$_7$))(μ_3-I)(μ_2-dppm)$_3$][I] (5). Following a method similar to the preparation of **3a**, **1a** (0.25 g, 0.16 mmol)

(25) Gong, J. K. Ph.D. Thesis, Purdue University, 1990.
(26) Gong, J. K.; Fanwick, P. E.; Kubiak, C. P. *J. Chem. Soc., Chem. Commun.* **1990**, 1190.

Table 3. Summary of Crystallographic Data for **1a**, **1a⁺**, and **2a**

	$1a\cdot3(CH_3C_6H_5)$	$[1a^+][CF_3SO_3]$	$[2a][PF_6]\cdot2(C_4H_8O)$
formula	$C_{96}H_{90}I_2Ni_3P_6$	$C_{76}H_{66}F_3I_2Ni_3O_3P_6S$	$C_{84}H_{82}F_3INi_3O_3P_7$
fw	1859.57	1732.21	1773.43
cryst size, mm	$0.30 \times 0.25 \times 0.22$	$0.63 \times 0.63 \times 0.13$	$0.50 \times 0.25 \times 0.06$
cryst system	triclinic	orthorhombic	monoclinic
space group	$P\bar{1}$	$Pnma$	$P2_1$
a, Å	15.116(2)	29.852(3)	10.847(2)
b, Å	16.016(3)	22.190(2)	26.068(7)
c, Å	19.957(2)	10.6564(9)	14.379(2)
α, deg	74.32(1)	90.0	90.0
β, deg	70.377(9)	90.0	98.76(2)
γ, deg	70.40(1)	90.0	90.0
V, Å³	4279(1)	7059(2)	4018(3)
Z	2	4	2
temp, °C	23	23	23
D_{calc}, g cm⁻³	1.443	1.630	1.473
μ, cm⁻¹	15.25	18.79	12.82
radiation (λ, Å)	Mo Kα (0.71073)	Mo Kα (0.71073)	Mo Kα (0.71073)
reflcns measd	11140 ($\pm h, \pm k, l$)	5175 ($+h, -k, +l$)	5399 ($\pm h, k, l$)
reflcns used	6494 with $I > 3\sigma(I)$	4000 with $I > 3\sigma(I)$	5386
variables	851	436	897
R	0.042	0.060	0.047
R_w	0.051[a]	0.080[a]	0.097[b]

[a] $R_w = [\sum w(F_o - F_c)^2/\sum wF_o^2]^{1/2}$. [b] $R_w = [\sum w(F_o^2 - F_c^2)^2/\sum w(F_o^2)^2]^{1/2}$.

and isopropyl isocyanide (0.11 g, 15 μL) gave **5**. Yield: 0.23 g (88%). ¹H NMR (CD₃CN): δ 4.75 (m, 1H, CNC*H*(CH₃)₂), 1.80 (d, 6H, CNCH-(C*H₃*)₂).

Preparation of [Ni₃(μ₃-CN(*t*-C₄H₉))(μ₃-I)(μ₂-dppm)₃][I] (6). Following a method similar to the preparation of **3a**, **1a** (1.0 g, 0.63 mmol) and *tert*-butyl isocyanide (0.052 g, 0.63 mmol) gave **6**. Yield: 0.72 g (76%). ¹H NMR (CD₃CN): δ 1.84 (s, 9H, CNC(C*H₃*)₃).

Preparation of [Ni₃(μ₃-CNC₆H₁₁)(μ₃-I)(μ₂-dppm)₃][I] (7). Following a method similar to the preparation of **3a**, **1a** (1.0 g, 0.63 mmol) and cyclohexyl isocyanide (0.068 g, 0.62 mmol) gave **7**. Yield: 0.67 g (72%). ¹H NMR (CD₃CN): δ 2.61 (m, 1H, C*H*), 2.35−2.00 (m, 8H, C*H₂*), 1.85 (m, 2H, C*H₂*).

Preparation of [Ni₃(μ₃-CNCH₂C₆H₅)(μ₃-I)(μ₂-dppm)₃][I] (8). Following a method similar to the preparation of **3a**, **1a** (1.0 g, 0.63 mmol) and benzyl isocyanide (0.073 g, 0.62 mmol) gave **8**. Yield: 0.57 g (61%). ¹H NMR (CD₃CN): δ 5.6 (m, 2H, C*H₂*C₆H₄).

Preparation of [Ni₃(μ₃-CNC₆H₅)(μ₃-I)(μ₂-dppm)₃][I] (9). Following a method similar to the preparation of **3a**, **1a** (0.37 g, 0.24 mmol) and phenyl isocyanide (0.027 g, 0.26 mmol) gave **9**. Yield: 0.29 g (74%).

Preparation of [Ni₃(μ₃-CN(*p*-C₆H₄I))(μ₃-I)(μ₂-dppm)₃][I] (10). Following a method similar to the preparation of **3a**, **1a** (1.0 g, 0.63 mmol) and *p*-iodophenyl isocyanide (0.14 g, 0.63 mmol) gave **10**. Yield: 0.52 g (60%).

Preparation of [Ni₃(μ₃-CN(*p*-C₆H₄Br))(μ₃-I)(μ₂-dppm)₃][I] (11). Following a method similar to the preparation of **3a**, **1a** (0.45 g, 0.28 mmol) and *p*-bromophenyl isocyanide (0.055 g, 0.30 mmol) gave **11**. Yield: 0.40 g (80%).

Preparation of [Ni₃(μ₃-CN(*p*-C₆H₄Cl))(μ₃-I)(μ₂-dppm)₃][I] (12). Following a method similar to the preparation of **3a**, **1a** (0.49 g, 0.31 mmol) and *p*-chlorophenyl isocyanide (0.043 g, 0.032 mmol) gave **12**. Yield: 0.40 g (75%).

Preparation of [Ni₃(μ₃-CN(*p*-C₆H₄F))(μ₃-I)(μ₂-dppm)₃][I] (13). Following a method similar to the preparation of **3a**, **1a** (1.0 g, 0.63 mmol) and *p*-fluorophenyl isocyanide (0.08 g, 0.66 mmol) gave **13**. Yield: 0.72 g (67%).

Preparation of [Ni₃(μ₃-CN(*p*-C₆H₄CH₃))(μ₃-I)(μ₂-dppm)₃][I] (14). Following a method similar to the preparation of **3a**, **1a** (0.50 g, 0.31 mmol) and *p*-methylphenyl isocyanide (0.038 g, 0.34 mmol) gave **14**. Yield: 0.35 g (65%). ¹H NMR (CD₂Cl₂): δ 2.55 (s, 3H, C₆H₄C*H₃*).

Preparation of [Ni₃(μ₃-CN(*p*-C₆H₄CF₃))(μ₃-I)(μ₂-dppm)₃][I] (15). Following a method similar to the preparation of **3a**, **1a** (1.0 g, 0.63 mmol) and *p*-(trifluoromethyl)phenyl isocyanide (0.11 g, 0.64 mmol) gave **15**. Yield: 0.48 g (43%).

Preparation of [Ni₃(μ₃-CN(*p*-C₆H₄OCH₃))(μ₃-I)(μ₂-dppm)₃][I] (16). Following a method similar to the preparation of **3a**, **1a** (0.30 g,

0.19 mmol) and *p*-methoxyphenyl isocyanide (0.027 g, 0.20 mmol) gave **16**. Yield: 0.24 g (74%). ¹H NMR (CD₂Cl₂): δ 4.06 (s, 3H, C₆H₄OC*H₃*).

Preparation of [Ni₃(μ₃-CN(*p*-C₆H₄CN))(μ₃-I)(μ₂-dppm)₃][I] (17). Following a method similar to the preparation of **3a**, **1a** (0.31 g, 0.20 mmol) and *p*-cyanophenyl isocyanide (0.028 g, 0.21 mmol) gave **17**. Yield: 0.26 g (78%). IR (KBr): ν(C≡N) = 2222 cm⁻¹.

Crystal Data Collection and Reduction for 1a. Crystals of **1a** were grown by slow diffusion of pentane into a toluene solution of **1a**. A dark green crystal was mounted in a glass capillary in a random orientation. The X-ray data were collected with an Enraf-Nonius CAD4 diffractometer with cluster **1a** crystallizing in the space group $P\bar{1}$ with two molecules of the complex and six molecules of toluene per unit cell. The crystal data and general conditions of data collection and structure refinement are given in Table 3. The positions of the nickel atoms were determined using the direct methods program SHELX-86[27a] and the remaining non-hydrogen atoms were located in difference Fourier maps after least-squares refinement. Reflection data were corrected for absorption using the method of Walker and Stuart.[28a] All H atoms were included at their idealized positions using sp³ or sp² geometry and were constrained to ride on the parent C atom. Selected bond distances and angles for **1a** are given in Table 4.

Crystal Data Collection and Reduction for 1a⁺. Crystals of **1a⁺** as a triflate salt were grown by slow diffusion of pentane into a dichloromethane solution of **1a⁺**. A dark purple crystal was mounted in a glass capillary in a random orientation. The X-ray data were collected with an Enraf-Nonius CAD4 diffractometer with cluster **1a⁺** crystallizing in the space group *Pnma*. The crystal data and general conditions of data collection and structure refinement are given in Table 3. The positions of the nickel atoms were determined using the direct methods program SHELX-86[27a] and the remaining non-hydrogen atoms were located in difference Fourier maps after least-squares refinement. Reflection data were corrected for absorption using the method of Walker and Stuart.[28a] All H atoms were included at their idealized positions using sp³ or sp² geometry and were constrained to ride on the parent C atom. Selected bond distances and angles for **1a⁺** are given in Table 5.

Crystal Data Collection and Reduction for 2a. Crystals of **2a** as the PF₆⁻ salt were obtained by diffusion of hexanes into a THF solution

(27) (a) Sheldrick, G. M. SHELXS-86. A Program for Crystal Structure Determination. Institüt für Anorganische Chemie der Univeristat Gottingen, 1986. (b) Sheldrick, G. M. SHELXS-93. A Program for Crystal Structure Determination. Institüt für Anorganische Chemie der Univeristat Gottingen, 1993.

(28) (a) Walker, N.; Stuart, D. *Acta Crystallogr.* **1983**, *A39*, 158. (b) Flack, H. D. *Acta Crystallogr.* **1983**, *A39*, 876.

Table 4. Selected Bond Distances (Å) and Angles (deg) for
$Ni_3(\mu_3-I)_2(\mu_2-dppm)_3 \cdot 3C_7H_8$ (**1a**·$3C_7H_8$)

Ni(1)−Ni(2)	2.474(2)	Ni(2)−I(1)	2.690(1)	Ni(1)−P(13)	2.187(3)
Ni(1)−Ni(3)	2.505(2)	Ni(2)−I(2)	2.745(1)	Ni(2)−P(21)	2.180(3)
Ni(2)−Ni(3)	2.480(2)	Ni(3)−I(1)	2.662(1)	Ni(2)−P(23)	2.187(3)
Ni(1)−I(1)	2.750(1)	Ni(3)−I(2)	2.721(1)	Ni(3)−P(31)	2.192(3)
Ni(1)−I(2)	2.694(1)	Ni(1)−P(12)	2.196(3)	Ni(3)−P(32)	2.195(3)
Ni(1)−Ni(2)−Ni(3)	60.75(5)	Ni(1)−Ni(2)−P(23)	156.90(9)		
Ni(2)−Ni(3)−Ni(1)	59.50(5)	Ni(1)−Ni(3)−P(32)	154.10(9)		
Ni(3)−Ni(1)−Ni(2)	59.75(5)	Ni(2)−Ni(1)−P(12)	96.85(8)		
I(1)−Ni(1)−I(2)	115.20(4)	Ni(2)−Ni(3)−P(31)	156.76(9)		
I(1)−Ni(2)−I(2)	115.55(5)	Ni(2)−Ni(1)−P(13)	154.55(9)		
I(1)−Ni(3)−I(2)	117.32(5)	Ni(2)−Ni(3)−P(32)	94.61(8)		
P(12)−Ni(1)−P(13)	108.4(1)	Ni(3)−Ni(1)−P(12)	156.22(9)		
P(21)−Ni(2)−P(23)	105.8(1)	Ni(3)−Ni(2)−P(21)	156.31(9)		
P(31)−Ni(3)−P(32)	108.0(1)	Ni(3)−Ni(1)−P(13)	94.83(8)		
Ni(1)−Ni(2)−P(21)	96.31(8)	Ni(3)−Ni(2)−P(23)	97.78(8)		
Ni(1)−Ni(3)−P(31)	97.83(8)				

Table 5. Selected Bond Distances (Å) and Angles (deg) for
$[Ni_3(\mu_3-I)_2(\mu_2-dppm)_3][CF_3SO_3]$ ($[\mathbf{1a^+}][CF_3SO_3]$)

Ni(1)−Ni(1)	2.503(2)	Ni(1)−I(2)	2.614(1)	Ni(1)−P(11)	2.237(3)
Ni(1)−Ni(2)	2.526(2)	Ni(2)−I(1)	2.635(2)	Ni(1)−P(12)	2.225(3)
Ni(1)−I(1)	2.668(1)	Ni(2)−I(2)	2.717(2)	Ni(2)−P(21)	2.221(3)
Ni(1)−Ni(1)−Ni(2)	60.30(3)	Ni(1)−Ni(1)−P(11)	96.17(8)		
Ni(1)−Ni(2)−Ni(1)	59.41(6)	Ni(1)−Ni(1)−P(12)	155.38(7)		
I(1)−Ni(1)−I(2)	114.30(5)	Ni(1)−Ni(2)−P(21)	97.60(7)		
I(1)−Ni(2)−I(2)	111.98(6)	Ni(1)−Ni(2)−P(21)	156.69(9)		
P(11)−Ni(1)−P(12)	108.3(1)	Ni(2)−Ni(1)−P(11)	156.10(9)		
P(21)−Ni(2)−P(21)	105.0(1)	Ni(2)−Ni(1)−P(12)	95.09(8)		

containing **2a** as an iodide salt and an excess of tetrabutylammonium hexafluorophosphate. A dark plate was mounted in a glass capillary in a random orientation. The X-ray data were collected with an Enraf-Nonius CAD4 diffractometer with cluster **2a** crystallizing with two molecules of **2a** and four molecules of THF per unit cell. The crystal data and general conditions of data collection and structure refinement are given in Table 3. The positions of the nickel atoms were determined using the direct methods program SHELX-93[27b] and the remaining non-hydrogen atoms were located in difference Fourier maps after least-squares refinement. An iodide atom on the carbonyl-capped face of **2a**, with its position derived from I(1) in **2a**, was also included due to the presence of $[Ni_3(\mu_3-I)_2(\mu_2-dppm)_3]^+[PF_6^-]$ (**1a⁺**) in the crystal lattice. The structure of **2a** was refined to give the iodide atom, I(2), and the carbonyl ligand, C(1) and O(1), at 8.6% and 91.4% occupancies, respectively. Reflection data were corrected for absorption using the method of Walker and Stuart.[28a] The absolute structure determination was determined by refinement of the Flack parameter, which refined to a value of 0.060(6).[28b] All H atoms were included at their idealized positions using sp^3 or sp^2 geometry and were constrained to ride on the parent C atom. Selected bond distances and angles for **2a** are given in Table 6.

Molecular Orbital Calculations. Extended Hückel MO calculations were carried out with use of the program CACAO (Computer Aided Composition of Atomic Orbitals).[29] Bis(diphenylphosphino)methane ligands were modeled as PH_3 and isocyanides were modeled as CNH. The $Ni_3(PH_3)_6$ core was arranged to have an ideal D_{3h} geometry. Nickel−nickel and nickel−ligand distances and angles were derived from structural information listed in Table 7.
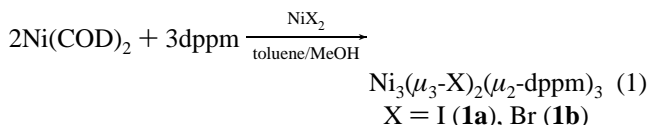
Results and Discussion

Synthesis of $Ni_3(\mu_3-I)_2(\mu_2-dppm)_3$ (1a). The cluster Ni_3-$(\mu_3-I)_2(\mu_2-dppm)_3$ (**1a**) serves as the parent of many of the carbonyl or isocyanide capped clusters reported here. A brief report of its synthesis[24] and photochemistry[17] has been published. Cluster **1a** is synthesized *via* a conproportionation of $Ni(COD)_2$ (COD = 1,5-cyclooctadiene) with NiI_2 in the presence of dppm. A similar procedure is utilized to generate the dibromide analog $Ni_3(\mu_3-Br)_2(\mu_2-dppm)_3$ (**1b**). The initial

Table 6. Selected Bond Distances (Å) and Angles (deg) for
$[Ni_3(\mu_3-CO)(\mu_3-I)(\mu_2-dppm)_3][PF_6] \cdot 2C_4H_8O$ ($[\mathbf{2a}][PF_6] \cdot 2C_4H_8O$)

Ni(1)−Ni(2)	2.408(3)	Ni(2)−I(2)	2.71(3)	Ni(1)−P(2)	2.189(6)
Ni(1)−Ni(3)	2.400(3)	Ni(2)−C(1)	1.90(2)	Ni(2)−P(3)	2.213(6)
Ni(2)−Ni(3)	2.397(2)	Ni(3)−I(1)	2.781(3)	Ni(2)−P(4)	2.207(6)
Ni(1)−I(1)	2.724(2)	Ni(3)−I(2)	2.79(3)	Ni(3)−P(5)	2.179(6)
Ni(1)−I(2)	2.73(3)	Ni(3)−C(1)	1.97(2)	Ni(3)−P(6)	2.196(6)
Ni(1)−C(1)	1.94(2)	Ni(1)−P(1)	2.227(5)	C(1)−O(1)	1.28(2)
Ni(2)−I(1)	2.735(3)				
Ni(1)−Ni(2)−Ni(3)	59.9(1)	Ni(1)−Ni(3)−P(6)	156.3(2)		
Ni(2)−Ni(3)−Ni(1)	60.3(1)	Ni(2)−Ni(1)−P(1)	96.8(2)		
Ni(3)−Ni(1)−Ni(2)	59.82(6)	Ni(2)−Ni(3)−P(5)	156.0(2)		
I(1)−Ni(1)−C(1)	104.6(5)	Ni(2)−Ni(1)−P(2)	155.0(2)		
I(1)−Ni(2)−C(1)	105.4(7)	Ni(2)−Ni(3)−P(6)	97.6(2)		
I(1)−Ni(3)−C(1)	101.8(6)	Ni(3)−Ni(1)−P(1)	156.4(2)		
P(1)−Ni(1)−P(2)	108.2(1)	Ni(3)−Ni(2)−P(3)	157.3(2)		
P(3)−Ni(2)−P(4)	104.7(2)	Ni(3)−Ni(1)−P(2)	95.2(2)		
P(5)−Ni(3)−P(6)	105.3(2)	Ni(3)−Ni(2)−P(4)	97.8(2)		
Ni(1)−Ni(2)−P(3)	98.1(2)	Ni(1)−C(1)−O(1)	141(2)		
Ni(1)−Ni(3)−P(5)	97.8(2)	Ni(2)−C(1)−O(1)	136(2)		
Ni(1)−Ni(2)−P(4)	156.6(2)	Ni(3)−C(1)−O(1)	124(2)		

reaction is between $Ni(COD)_2$ and dppm in toluene to produce a red-orange intermediate. This intermediate is incompletely characterized but has frequently been employed by Shaw and co-workers as well as by our group to produce a variety of $d^{10}-d^{10}$ and d^9-d^9 binuclear nickel complexes.[26,30,31] The most reasonable assignment of the structure of the Ni(0)−dppm intermediate involved, by analogy to the well-characterized species $Pd_2(\mu_2-dppm)_3^{32-34}$ and $Pt_2(\mu_2-dppm)_3$,[35,36] is the dimeric species $Ni_2(\mu_2-dppm)_3$. Most previous reactions leading to trinuclear nickel clusters have involved reaction of $d^{10}-d^{10}$ binuclear complexes with Ni(II) compounds or halocarbons.[9,10] Consistent with this synthetic approach, the addition of an alcoholic solution of anhydrous NiX_2 (X = I, Br; 0.5 equiv *vs* $Ni(COD)_2$) to the putative $Ni_2(\mu_2-dppm)_3$ leads to the instantaneous formation of **1a** or **1b**, as a dark green or brown solid, respectively (eq 1).

$$2Ni(COD)_2 + 3dppm \xrightarrow[\text{toluene/MeOH}]{NiX_2}$$

$$Ni_3(\mu_3-X)_2(\mu_2-dppm)_3 \quad (1)$$
$$X = I \ (\mathbf{1a}), \ Br \ (\mathbf{1b})$$

Clusters **1a** and **1b** are isolated as analytically pure solids but may be recrystallized from hot toluene after filtration through Celite. Attempts to make $Ni_3(\mu_3-Cl)_2(\mu_2-dppm)_3$ from an analogous reaction with $NiCl_2$ were unsuccessful; other avenues for the synthesis of $Ni_3(\mu_3-Cl)_2(\mu_2-dppm)_3$ are currently being pursued.
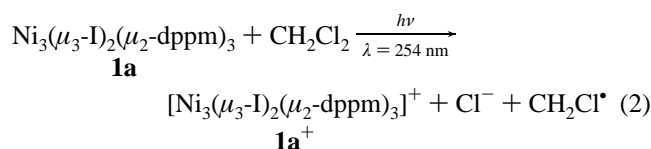
Oxidation of 1. Clusters **1a** and **1b** may be oxidized to their monocations $[Ni_3(\mu_3-X)_2(\mu_2-dppm)_3]^+$(X = I (**1a⁺**), Br (**1b⁺**)) by a variety of reagents including iodine and silver or ferrocenium salts. Use of excess oxidant does not lead to further oxidation. The cluster cation **1a⁺** has an intense purple color (λ_{max} = 563.2 nm, ϵ = 12.6 × 10^3 $M^{-1} \cdot cm^{-1}$) and is air-stable in the solid state. The oxidation of **1a** may also be accomplished by irradiation of a solution of **1a** in methylene chloride or chloroform (eq 2).

(29) Mealli, C.; Proserpio, D. M. *J. Chem. Educ.* **1990**, *67*, 399.

(30) Gong, J. K.; Kubiak, C. P. *Inorg. Chim. Acta* **1989**, *162*, 19.
(31) Fontaine, X. L. R.; Higgins, S. J.; Shaw, B. L.; Thornton-Pett, M.; Yichang, W. *J. Chem. Soc., Dalton Trans.* **1987**, 1501.
(32) Caspar, J. V. *J. Am. Chem. Soc.* **1985**, *107*, 6718.
(33) Stern, E. W.; Maples, P. K. *J. Catal.* **1972**, *27*, 120.
(34) Stern, E. W.; Maples, P. K. *J. Catal.* **1972**, *27*, 134.
(35) Chin, C.-S.; Sennett, M. S.; Weir, P. J.; Vaska, L. *Inorg. Chim. Acta* **1978**, *31*, L443.
(36) Manojlović-Muir, L.; Muir, K. W.; Grossel, M. C.; Brown, M. P.; Nelson, C. D.; Yavari, A.; Kallas, E.; Moulding, R. P.; Seddon, K. R. *J. Chem. Soc., Dalton Trans.* **1986**, 1955.

Table 7. Comparison of Bond Distances and Angles of Iodide-Capped Nickel Trimers
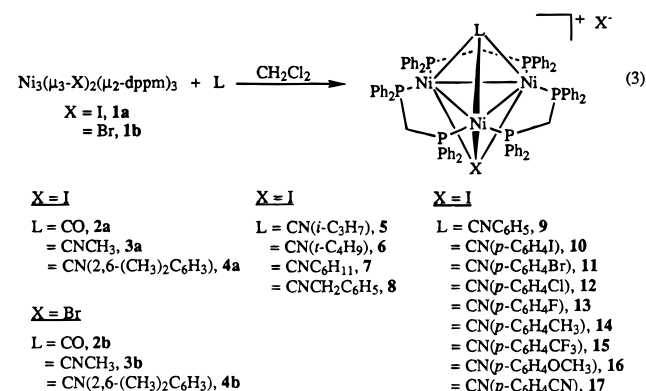
compd	d_{Ni-Ni} (Å)	d_{Ni-I} (Å)	d_{Ni-C} (Å)	d_{Ni-P} (Å)	$\angle_{P-Ni-P}$ (deg)
Ni$_3$(μ_3-I)$_2$(μ_2-dppm)$_3$ (**1a**)	2.49(2)	2.70(3)		2.19(1)	107.4(8)
[Ni$_3$(μ_3-I)$_2$(μ_2-dppm)$_3$]$^+$ (**1a$^+$**)	2.52(1)	2.65(4)		2.23(1)	107.2(16)
[Ni$_3$(μ_3-CO)(μ_3-I)(μ_2-dppm)$_3$]$^+$ (**2a**)	2.40(1)	2.75(2)	1.94(2)	2.20(2)	106.0(11)
[Ni$_3$(μ_3-CNCH$_3$)(μ_3-I)(μ_2-dppm)$_3$]$^+$ (**3a**)^a	2.42(2)	2.75(3)	2.01(1)	2.20(1)	105.2(4)

^{a} Ratliff, K. S.; Fanwick, P. E.; Kubiak, C. P. *Polyhedron* **1990**, *9*, 1487.

$$\text{Ni}_3(\mu_3\text{-I})_2(\mu_2\text{-dppm})_3 + \text{CH}_2\text{Cl}_2 \xrightarrow[\lambda = 254 \text{ nm}]{h\nu}$$
$$\textbf{1a}$$

$$[\text{Ni}_3(\mu_3\text{-I})_2(\mu_2\text{-dppm})_3]^+ + \text{Cl}^- + \text{CH}_2\text{Cl}^\bullet \quad (2)$$
$$\textbf{1a}^+$$

Photooxidation of **1a** to **1a$^+$** is accompanied by the reduction of methylene chloride to chloride and chloromethyl radical.[17] The course of the photooxidation of **1a** by CH$_2$Cl$_2$ can be monitored by UV–vis spectroscopy. The photooxidation (550 W Hg lamp) is complete in several minutes and is accompanied by a clean isosbestic transformation from **1a** to **1a$^+$**. Outer-sphere photoreduction of methylene chloride requires potentials negative of −2.4 V *vs* SCE.[37] The preservation of the trinuclear structure through the course of photooxidation of **1a** by CH$_2$-Cl$_2$ to **1a$^+$** can be attributed to the presence of multiple bridging dppm and iodide ligands. In fact, the trinuclear structure of these clusters is maintained under electrochemical[14−16] and mass spectrometric[24] conditions and also through capping ligand substitutions (*vide infra*). The photoinduced charge transfer properties and structural stabilities of **1a** and **1a$^+$** have been employed to effect the reduction of CO$_2$ directly to the carbon dioxide radical anion, CO$_2$$^{\bullet-}$.[17] Traces of **1a$^+$** dramatically broaden the ^{31}P NMR spectrum of **1a** in solvents that dissolve both oxidation states, such as THF and CH$_2$Cl$_2$. The broadening is attributed to self-exchange electron transfer as the addition of a small amount of sodium naphthalenide or sodium borohydride to a THF solution of **1a/1a$^+$** sharpens the ^{31}P NMR spectrum to a narrow singlet at −14.0 ppm. Both **1a** and **1a$^+$** have been characterized by X-ray diffraction (*vide infra*).

Synthesis of Carbonyl- and Isocyanide-Capped Nickel Clusters. While substitution of terminal ligands in clusters is common and has been extensively studied,[38] direct substitution of face-bridging ligands is unusual.[39] Dahl and co-workers reported that [Co$_3$Cp$_3$(μ_3-CO)(μ_3-NH)] could be converted to [Co$_3$Cp$_3$(μ_3-NO)(μ_3-NH)]$^+$ by reaction with NO[BF$_4$].[40] Substitution of one of the capping halides of **1** by a variety of π-acceptor ligands proved to be facile at room temperature (Eq 3). The conversions are quantitative and, although the substitution of a second halide is not observed, only a stoichiometric amount of isocyanide ligand is added to avoid the formation of side products.

Figure 1. Cyclic voltammogram of a 1.0 mM solution of [Ni$_3$(μ_3-CN(p-C$_6$H$_4$OCH$_3$))(μ_3-I)(μ_2-dppm)$_3$][PF$_6$] (**16**) in CH$_3$CN with 0.1 M TBAP as supporting electrolyte.

the product is the previously reported cluster [Ni$_3$(μ_3-CNCH$_3$)-(μ_3-I)(μ_2-dppm)$_3$]$^+$ (**3a**).[9,15] All of the clusters **2−17** were characterized spectroscopically and, additionally, **2a** was characterized by X-ray diffraction. The clusters reported have remarkably similar UV–vis and ^{31}P spectra and can be reversibly reduced at similar potentials, *ca.* −1.1 V *vs* SCE, as summarized in Tables 1 and 2. The rather large cathodic potentials required for reduction are attributed to the stability of the 48-electron clusters (counting iodide as a six-electron donor) as reduction generates a 49-electron neutral cluster (*vide infra*). The cyclic voltammogram of **16**, which is representative of the carbonyl and isocyanide clusters, is shown in Figure 1. The reversible nature of the single electron reduction of these clusters is readily apparent from their cyclic voltammograms. A useful technique for the identification of the clusters is plasma desorption (PD) mass spectrometry as the molecular ion is observed for each cluster (Table 2). A complete analysis of the fragmentation patterns and matrix effects observed has been reported separately.[24]

Cluster **3a**, generated from the reaction of CNCH$_3$ and Ni$_3$-(μ_3-I)$_2$(μ_2-dppm)$_3$, has been reported previously.[9,15] However, this complex was initially synthesized *via* the reaction of Ni$_2$-(μ_2-dppm)$_2$(μ_2-CNCH$_3$)(CNCH$_3$)$_2$ with CH$_2$I$_2$. A similar synthetic strategy was used to synthesize the bromide congener, [Ni$_3$(μ_3-CNCH$_3$)(μ_3-Br)(μ_2-dppm)$_3$][Br], whereby Ni$_2$(μ_2-dppm)$_2$-(μ_2-CNCH$_3$)(CNCH$_3$)$_2$ and NiBr$_2$ were utilized to form **3b**. Of note is that **3b** can also be prepared *via* the reaction of CNCH$_3$ with Ni$_3$(μ_3-Br)$_2$(μ_2-dppm)$_3$ (eq 3). The bromide−carbonyl capped cluster (**2a**) was prepared using a method first outlined by Puddephatt and co-workers in the synthesis of [Ni$_3$(μ_3-CO)-(μ_3-Cl)(μ_2-dppm)$_3$][Cl].[10] Specifically, thermal disproportionation of Ni$_2$(μ_2-dppm)$_2$(μ-CO)Br$_2$ produced [Ni$_3$(μ_3-CO)(μ_3-Br)(μ_2-dppm)$_3$][Br] (**2b**) in good yield.

Structural Aspects of Iodide-Capped Nickel Trimers. Interpretation of X-ray structural data for clusters is frequently complicated by considerations of site symmetry.[40,41] All of the clusters reported here have a nominal C$_3$ axis passing through the capping ligands and disorder about this axis can give rise to an apparent crystallographic C$_3$ axis which disguises the true

$$\text{Ni}_3(\mu_3\text{-X})_2(\mu_2\text{-dppm})_3 + \text{L} \xrightarrow{\text{CH}_2\text{Cl}_2} \quad (3)$$

X = I, **1a**
= Br, **1b**

X = I

L = CO, **2a**
= CNCH$_3$, **3a**
= CN(2,6-(CH$_3$)$_2$C$_6$H$_3$), **4a**

X = I

L = CN(i-C$_3$H$_7$), **5**
= CN(t-C$_4$H$_9$), **6**
= CNC$_6$H$_{11}$, **7**
= CNCH$_2$C$_6$H$_5$, **8**

X = I

L = CNC$_6$H$_5$, **9**
= CN(p-C$_6$H$_4$I), **10**
= CN(p-C$_6$H$_4$Br), **11**
= CN(p-C$_6$H$_4$Cl), **12**
= CN(p-C$_6$H$_4$F), **13**
= CN(p-C$_6$H$_4$CH$_3$), **14**
= CN(p-C$_6$H$_4$CF$_3$), **15**
= CN(p-C$_6$H$_4$OCH$_3$), **16**
= CN(p-C$_6$H$_4$CN), **17**

X = Br

L = CO, **2b**
= CNCH$_3$, **3b**
= CN(2,6-(CH$_3$)$_2$C$_6$H$_3$), **4b**

When CNCH$_3$ is used to effect substitution of an iodide ligand,

(37) Hawley, M. D. In *Encyclopedia of the Electrochemistry of the Elements*; Bard, A. J., Ed.; Marcel Dekker: New York, 1973; Vol. 14, p 24.

(38) Darensbourg, D. J. In *The Chemistry of Metal Cluster Complexes*; Shriver, D. F., Kaesz, H. D., Adams, R. D., Eds.; VCH: New York, 1990; p 171.

(39) Band, E.; Muetterties, E. L. *Chem. Rev.* **1978**, *78*, 639.

(40) Bedard, R. L.; Rae, A. D.; Dahl, L. F. *J. Am. Chem. Soc.* **1986**, *108*, 5924.

(41) Tsuge, K.; Yajima, S.; Imoto, H.; Saito, T. *J. Am. Chem. Soc.* **1992**, *114*, 7910.
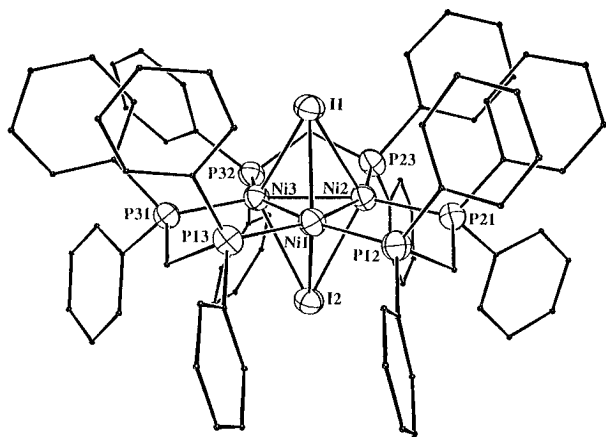
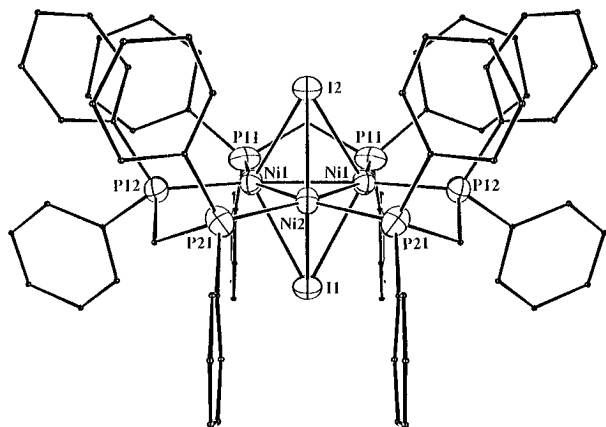**Figure 2.** ORTEP view of $Ni_3(\mu_3\text{-}I)_2(\mu_2\text{-}dppm)_3$ (**1a**).

Figure 3. ORTEP view of $[Ni_3(\mu_3\text{-}I)_2(\mu_2\text{-}dppm)_3]^+$ (**1a**$^+$). $CF_3SO_3^-$ counterion not shown.
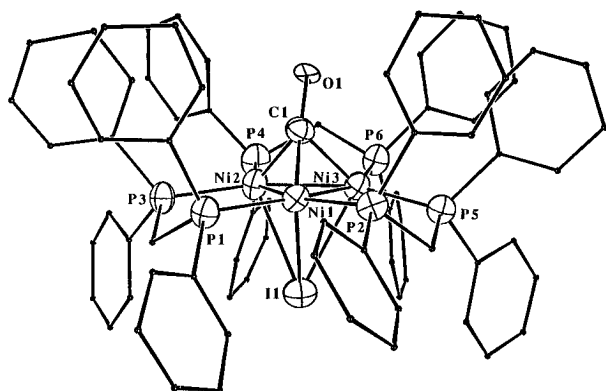

Figure 4. ORTEP view of $[Ni_3(\mu_3\text{-}CO)(\mu_3\text{-}I)(\mu_2\text{-}dppm)_3]^+$ (**2a**). PF_6^- counterion not shown.

symmetry of the molecule. However, none of the clusters reported in Table 3 possess C_3 site symmetry in the crystalline form. The ORTEP diagrams for $Ni_3(\mu_3\text{-}I)_2(\mu_2\text{-}dppm)_3$ (**1a**), $[Ni_3\text{-}(\mu_3\text{-}I)_2(\mu_2\text{-}dppm)_3]$ (**1a**$^+$), and $[Ni_3(\mu_3\text{-}CO)(\mu_3\text{-}I)(\mu_2\text{-}dppm)_3]^+$ (**2a**) are shown in Figures 2, 3, and 4, respectively. A comparison of selected bond distances and angles for **1a**, **1a**$^+$, and **2a** appears in Table 7.

The three nickel–nickel bonds in **1a** and **2a** are crystallographically independent and the metal triangle is essentially equilateral with an average Ni–Ni distance of 2.49(2) Å in **1a** and an average Ni–Ni separation of 2.40(1) Å in **2a**. In contrast, $[Ni_3(\mu_3\text{-}I)_2(\mu_2\text{-}dppm)_3]^+$ (**1a**$^+$) crystallizes in the orthorhombic space group *Pnma* and the triangle of nickel atoms is bisected by one of the crystallographic mirror planes. The metal atoms thus form an isosceles structure with two long sides

(d_{Ni-Ni} = 2.526(2) Å) and one short side (d_{Ni-Ni} = 2.503(2) Å). The lowering of the molecular symmetry of **1a** from D_{3h} to C_{2v} upon oxidation to **1a**$^+$ is consistent with a degenerate ground state (*vide infra*). The removal of one electron from the doubly degenerate HOMO of **1a** to form **1a**$^+$ results in a Jahn–Teller distortion, which would manifest itself as inequivalent Ni–Ni bond lengths in **1a**$^+$. The average bond length is only slightly affected by the oxidation, consistent with a HOMO that is essentially nonbonding with respect to the trinickel core (*vide infra*).

The parameters listed in Table 7 reveal other structural trends. The average nickel–nickel bond distances of the two diiodo bridged clusters, **1a** and **1a**$^+$, are longer than those in the CO (**2a**) or $CNCH_3$[9] (**3a**, average d_{Ni-Ni} = 2.42(2) Å) capped clusters, a difference of approximately 0.09 Å. This lends support to the assignment of **1a** as a 52-electron species. Increases in electron count in trinuclear metal clusters above a cluster valence electron count of 48 are inevitably accompanied by an increase in metal–metal bond distances. The mean metal–metal distance in the 49-electron cluster $[Co_3(CO)_9(\mu_3\text{-}S)]$ is 0.083 Å longer than that observed for its 48-electron counterpart $[FeCo_2(CO)_9(\mu_3\text{-}S)]$.[42] Conversely, Dahl and coworkers have shown that oxidation of the 48-electron cluster $[Co_3Cp^*_3(\mu_3\text{-}CO)(\mu_3\text{-}NH)]$ to its 47-electron monocation causes a minimal decrease of 0.019 Å in the average metal–metal distance.[43] Alternatively, the shortening of the Ni–Ni distances in **2a** and **3a**, as compared to **1a** and **1a**$^+$, may also be attributed to steric factors. The replacement of a large capping iodide (**1a**, **1a**$^+$) with smaller CO (**2a**) or $CNCH_3$ (**3a**) ligands could conceivably lead to a compression of the Ni–Ni distances in the trinuclear nickel core in order to maximize Ni–CO or Ni–$CNCH_3$ overlap. Thus, electronic and steric effects may be used to account for the differences in Ni–Ni bond lengths.

Triply-bridging iodide ligands tend to stabilize clusters with weak nickel–nickel bonds. In 1979, Stone tabulated a comparison of nickel–nickel bond lengths in dimers and clusters.[44] All of the nickel–nickel distances which could be described as bonding were in the range 2.35–2.47 Å; nonbonding interactions corresponded to distances above 2.64 Å. If we restrict our attention to clusters of three nickel atoms or more, only two crystallographically characterized examples of nickel–nickel bond distances between 2.47 and 2.7 Å have been reported. These are clusters **1a** and $[Ni_3(PPh_3)_3(\mu_3\text{-}I)(\mu_2\text{-}I)_3]$, reported by Hoberg and co-workers,[45] which have average nickel–nickel bond lengths of 2.52(1) and 2.655(2) Å, respectively. Both compounds possess a triply-bridging iodide, but in the case of **1a**, the presence of bridging dppm ligands likely accounts for the shorter observed Ni–Ni bond distances.[1]

The average Ni–I bond lengths in **1a** (2.70(3) Å) and **1a**$^+$ (2.65(4) Å) are slightly shorter than those in **2a** and **3a**, (2.75-(2) and 2.75(3) Å). The bonding between triply-bridging ligands and the metal framework is complex in clusters, involving both π- and σ-symmetry hybrid ligand orbitals interacting with a_1 and e orbitals of the metal fragment.[46] Dahl and co-workers recently reported that the C–O and C–S bond lengths in the series of clusters $[Ni_3(\mu_3\text{-}L)(\mu_3\text{-}L')Cp_3]$, (L, L' = CO, CS) showed evidence that the axial ligands competed for π-electron density donated by the metal framework.[47] The small observed

(42) Stevenson, D. L.; Wei, C. H.; Dahl, L. F. *J. Am. Chem. Soc.* **1971**, *93*, 6027.

(43) Ziebarth, M. S.; Dahl, L. F. *J. Am. Chem. Soc.* **1990**, *112*, 2411.

(44) Davidson, J. L.; Green, M.; Stone, F. G. A.; Welch, A. J. *J. Chem. Soc., Dalton Trans.* **1979**, 506.

(45) Hoberg, J.; Radine, K.; Kruger, C.; Romao, M. J. *Z. Naturforsch.* **1985**, *40b*, 607.

(46) Schilling, B. E. R.; Hoffmann, R. *J. Am. Chem. Soc.* **1979**, *101*, 3456.
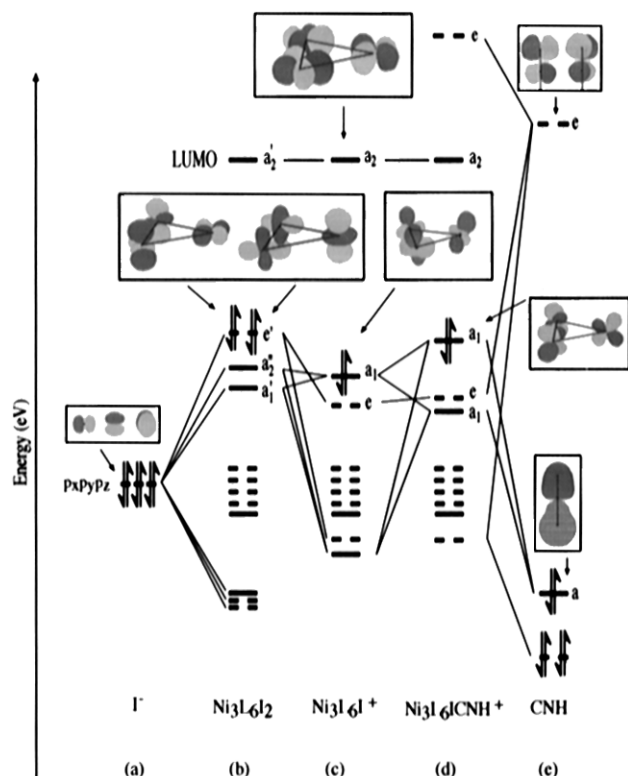
Figure 5. Interaction diagram for $Ni_3(I)_2(PH_3)_6$ (b) and $[Ni_3(CNH)-(I)(PH_3)_6]^+$ (d) derived from iodide (a), $[Ni_3(I)(PH_3)_6]^+$ (c), and CNH (e) fragments. Only Ni-based orbitals in the HOMO and LUMO are shown.

Ni−I bond distance changes may be rationalized by arguing that π-acceptor ligands such as CO and CNCH₃ interact more strongly with π-symmetry metal fragment orbitals than does the π-donating iodide ligand. Hence, replacement of one capping iodide with CO or CNCH₃ tends to weaken metal−ligand bonding to the remaining triply-bridging iodide. Additionally, steric effects may contribute to the observed lengthening of the Ni−I bonds in **2a** and **3a**. The smaller trinuclear nickel cores in **2a** and **3a** would result in reduced Ni−I overlap, lengthening the Ni−I bonds in **2a** and **3a** compared to those of **1a** and **1a⁺**. Thus, steric and electronic effects cannot clearly differentiate trends in Ni−Ni or Ni−I bonding.

Molecular Orbital Calculations. Bonding schemes for trinuclear clusters with either ML₃[40,46,48] or ML₂[49] vertices have been discussed by other workers, but the specific types of compounds reported in this paper (52-electron clusters with π-donating ligands) have not been treated. We are interested in relating the electronic structure of **1** and **2−17** to their spectroscopic properties and reactivity. Results of Extended Hückel MO calculations on these compounds are presented (Figure 5). The bonding scheme was constructed by adding an iodide or isocyanide, modeled as HNC, to the fragment $Ni_3L_6I^+$. The dppm ligands were modeled as six PH₃ ligands arranged in the same geometry as the dppm phosphorus atoms. The MO diagrams for $Ni_3I_2(PH_3)_6$ and $[Ni_3(CNH)(I)(PH_3)_6]^+$ are shown in Figure 5.

(47) North, T. E.; Thoden, J. B.; Spencer, B.; Bjarnson, A.; Dahl, L. F. *Organometallics* **1992**, *11*, 4326.

(48) (a) Maj, J. J.; Rae, A. D.; Dahl, L. F. *J. Am. Chem. Soc.* **1982**, *104*, 3054. (b) Rives, A. B.; Xiao-Zeng, Y.; Fenske, R. F. *Inorg. Chem.* **1982**, *21*, 2286.

(49) (a) Evans, D. G.; Mingos, D. M. *J. Organomet. Chem.* **1982**, *240*, 321. (b) Mealli, C. *J. Am. Chem. Soc.* **1985**, *107*, 2245. (c) Evans, D. G. *J. Organomet. Chem.* **1988**, *335*, 397. (d) Puddephatt, R. J.; Xioa, J.; Kristof, E.; Vittal, J. *J. Organomet. Chem.* **1995**, *490*, 1.

Figure 5 emphasizes the differences between clusters containing the π-accepting isocyanide ligand or the π-donating iodide. The latter system clearly has a filled doubly-degenerate HOMO. We also find[50] that when Te²⁻ is substituted for I⁻ to form Ni₃-(μ₃-Te)₂(μ₂-dppm)₃, the resulting ditelluride trimer is paramagnetic. This observation is consistent with a half-filled e′ level (HOMO) in the 50-electron ditelluride complex, compared to the completely filled HOMO in the 52-electron diiodide cluster, **1a**. The HOMO in $Ni_3I_2(PH_3)_6$ is antibonding with respect to the Ni−Ni bonds, and a small decrease in average Ni−Ni bond length when **1a** is oxidized to **1a⁺** (Table 7) is consonant with the calculated MO scheme. The odd-electron diiodide cluster **1a⁺** had no detectable EPR spectrum at room temperature in solution or in frozen solution (100 K). This also supports a doubly degenerate (e′) HOMO for **1a**. Rapid spin relaxation is expected in a species such as **1a⁺** in which the unpaired electron occupies a pair of degenerate orbitals, resulting in a broadened signal. Previous workers[51] have found such broadening in [Co₃-Cp₃(μ₃-CPh)₂]⁺ and Ziebarth and Dahl did not observe an EPR signal for [Co₃Cp*₃(μ₃-CO)(μ₃-NH)]⁺ down to 100 K.[42]

For the isocyanide derivatives **3−17** it appears that a stronger σ interaction and weaker π interaction with the isocyanide compared to the iodide leads to a HOMO of a₂ symmetry. The inherently approximate nature of the calculations leaves this conclusion open to question in the absence of corroborating experimental information. However, Fenske and co-workers, in their theoretical study of (ML₃)₃ clusters, reached a similar conclusion.[48b] The LUMO in complexes **1−17** is composed of in-plane nickel d orbitals of a₂ symmetry. The energy of the LUMO is little changed by the addition of capping ligands since they possess no fragment molecular orbitals of like symmetry. According to Figure 5, the addition of an electron to the CNR or CO derivatives should have little effect on the capping ligands. Infrared spectroelectrochemical studies have shown that the capping carbonyl or isocyanide ligands remain μ₃-η¹ upon reduction, although there is a significant shift of ν(C≡N) or ν(C≡O) to lower frequency.[16] It is interesting to note that in other trinuclear clusters studied by Dahl and co-workers, a similar effect was observed as the reduction of [Ni₃-(η⁵-C₅H₅)₃(μ-CO)₂] to the monoanion caused a 30-cm⁻¹ decrease in ν(CO); for [(η⁵-C₅Me₅)CoNi₂(η⁵-C₅H₅)(μ₃-CO)₂], a decrease of 45 cm⁻¹ was observed.[48a] In these clusters, despite the differences due to the presence of cyclopentadienyl ligands instead of bis-phosphines, calculations show that the frontier orbitals include an a₂ MO of very similar characteristics to the one described for [Ni₃(CNH)(I)(PH₃)₆]⁺. In both [(η⁵-C₅Me₅)-CoNi₂(η⁵-C₅H₅)(μ₃-CO)₂] and [Ni₃(CNH)(I)(PH₃)₆]⁺ the a₂ orbital is the LUMO. Thus, in each case, single electron reduction increases the occupancy of this molecular orbital. The weakening of the C−O bond in [(η⁵-C₅Me₅)CoNi₂(η⁵-C₅H₅)-(μ₃-CO)₂] was explained by Dahl as being due to a raising of the nickel core d orbital energies by the additional charge, leading to more effective metal−CO π* back-bonding. The assignment of an a₂ LUMO to **2−17** is supported by EPR spectroscopy. Clusters **2a** and **3a** both exhibit symmetric septet solution EPR spectra when reduced by one electron with sodium naphthelenide in THF with *g* factors of 2.065 and 2.067, respectively. Coupling to the phosphorus nuclei is large (54.5 and 60.8 G), consistent with the prediction that the largely metal-based LUMO's of **2a** and **3a** lie in the plane containing the metal triangle and phosphorus nuclei (*vide supra*).

(50) Ferrence, G. M.; Fanwick, P. E.; Kubiak, C. P. *J. Chem. Soc., Chem. Commun.* Submitted for publication.

(51) Enoki, S.; Kawamura, T.; Yonezawa, T. *Inorg. Chem.* **1983**, *22*, 3821.

Electrochemistry of Trinuclear Nickel Clusters. Differences between π-Acceptor and π-Donor Capping Ligands. The electrochemistry of the nickel clusters provides evidence of a dramatic effect of substituting a π-acceptor capping ligand for a π-donor. All of the CO and isocyanide capped clusters **2−17** exhibit strikingly similar cyclic voltammetric properties. As shown in Table 2, **2−17** all undergo a reversible single-electron reduction at *ca.* −1.1 V *vs* SCE in acetonitrile. This reductive couple corresponds to adding an additional electron to a 48-electron cluster, hence the comparatively cathodic potential at which it occurs. Peak-to-peak separations are less than 80 mV in all cases. Cluster **3a** is a known electrocatalyst for the reduction of CO_2,[15,16,52] and the ease with which analogs may be prepared allowed it to be expanded into a family of electrocatalysts. However, little variation in the voltammetric properties is observed. This is most evident in Table 2, where it is shown that changing from alkyl (**3, 5−8**) to aryl (**4, 9−17**) isocyanides has negligible effects on the values of $E_{1/2}(0/+)$. In addition, varying the substituents in a series of *para*-substituted phenyl isocyanide-capped nickel clusters resulted in negligible changes in electrochemical properties. Control of the electrochemical properties of cobalt clusters by variation of the capping ligand has been demonstrated.[53] However, in the clusters studied here, the largely metal localized nature of the a_2 LUMO accounts well for the limited variation in $E_{1/2}(0/+)$ with capping ligand.

The electrochemistry of the dihalide-capped clusters **1/1$^+$** does not conform to the pattern established by the clusters **2−17**. For **1a**, two reversible oxidations at −0.68 and −0.19 V *vs* SCE are seen. No reduction wave is observed as far negative as −2.0 V *vs* SCE. Clearly, **1a** should not be regarded as an analog of **2a**, **3a**, **4a**, or **5−17** with the simple replacement of a CO or isocyanide by an iodide. The substitution of an iodide for an isocyanide is accompanied by a significant electronic change in the molecule concomitant with the transformation from a 48- to a 52-electron cluster. Also, clusters **2−17** carry a positive charge which enables them to be more easily reduced.

Fermi Resonance in Symmetric (μ_3-η^1) Bridging Isocyanide Ligands. The most prominent FT-IR features of the isocyanide-capped nickel clusters reported here are the C≡N stretching bands of the capping isocyanide ligands. In the compounds studied, *two* ν(C≡N) bands were observed in the infrared spectra (KBr pellets), contrary to the expected single band (Table 2). Puddephatt and co-workers reported two ν(C≡N) bands (KBr pellet) at 1989 and 1968 cm^{-1} for Pd_3-$(\mu_2$-dppm$)_3(\mu_3$-CN(2,6-Me$_2$C$_6$H$_3$))$^{2+}$ and attributed the two-band pattern to matrix effects in the solid state, as only one band at 1972 cm^{-1} was observed in CH_2Cl_2 solution.[54] For the alkyl-substituted isocyanide complexes (**3, 5−8**), the ν(C≡N) bands are too weak and broad to be observed in solution. However, for the aryl-substituted species (**4, 9−17**), two ν(C≡N) bands can be observed in THF solution. For example, [Ni$_3(\mu_3$-CN-(2,6-Me$_2$C$_6$H$_3$))$(\mu_3$-I)$(\mu_2$-dppm$)_3$][I] (**4a**) shows two ν(C≡N) bands in THF solution at 1849 and 1822 cm^{-1}, the same as observed in the solid state (KBr pellet). This effectively rules out the possibility that matrix effects are accounting for the observation of two ν(C≡N) bands in this class of isocyanide-capped nickel clusters.

Other possible sources of the two-band phenomenon were considered. The presence of two different isomers was not consistent with X-ray crystallographic results. For **3a**, only one cluster per asymmetric unit was observed yet this species still
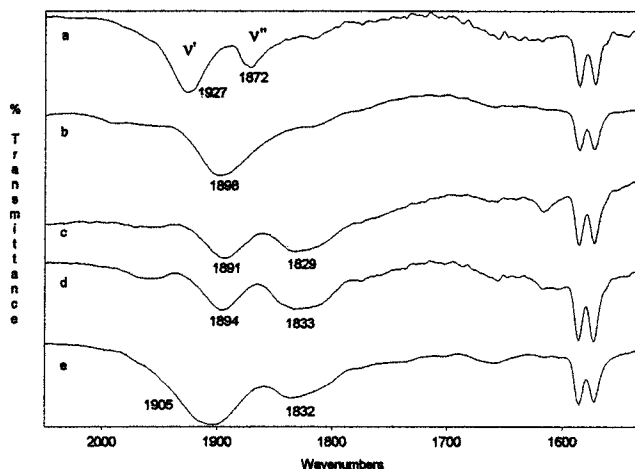

Figure 6. Solid state FT-IR spectra of isotopically labeled [Ni$_3(\mu_3$-CNCH$_3)(\mu_3$-I)$(\mu_2$-dppm$)_3$]$^+$. (a) CNCH$_3$ (**3a**). (b) CNCD$_3$ (**3a-CD$_3$**). (c) ^{13}CNCH$_3$ (**3a-^{13}C**). (d) C^{15}NCH$_3$ (**3a-^{15}N**). (e) CN^{13}CH$_3$ (**3a-^{13}CH$_3$**).

retains its distinctive two ν(C≡N) band pattern.[9] A Jahn−Teller distortion was deemed unlikely on the basis of molecular orbital calculations (*vide supra*) and nondegenerate ground states of **2−17**. The HOMO levels of these isocyanide-capped clusters are of a_2 symmetry and are completely filled, removing the driving force for distortion.[55] Also, in the solid state structure of **3a**, no distortion was evident as no significant differences in Ni−Ni bond distances and angles were observed. The presence of a "hot band" was rejected as the IR spectrum of **4a** (KBr pellet) remained unchanged down to *ca.* 40 K.[56,57] A combination band involving the ν(Ni−I) fundamental was not compatible with the observation of two ν(C≡N) bands for the isocyanide clusters containing a bromide cap (**3b, 4b**).[57]

The effects of Fermi resonance were considered in detail. Fermi resonance is defined as the mixing of a fundamental band with an overtone (or combination) band of the same symmetry.[58,59] In Fermi resonance, the intensity of the fundamental is shared with the overtone resulting in the appearance of two bands. Fermi resonance is only possible when the fundamental and the overtone *both* have the same symmetry and are close in energy. To investigate Fermi resonance effects, a series of isotopically labeled methyl isocyanide capped nickel clusters were synthesized using CNCH$_3$ (**3a**), ^{13}CNCH$_3$ (**3a-^{13}C**), C^{15}NCH$_3$ (**3a-^{15}N**), CN^{13}CH$_3$ (**3a-^{13}CH$_3$**), and CNCD$_3$ (**3a-CD$_3$**). All of these clusters were analyzed using ^{31}P NMR spectroscopy and electrochemistry and were found to be similar to the parent cluster **3a**. The IR spectra of the various methyl isocyanide capped clusters are shown in Figure 6. The frequencies of the ν(C≡N) bands are listed in Table 8. Most striking is the observation of a *single* ν(C≡N) band for the CNCD$_3$-capped cluster (**3a-CD$_3$**) and *two* variously shifted ν-(C≡N) bands for the remaining isotopomers. If the spectrum of **3a-CD$_3$** represents the non-resonant condition, then inspection of the IR spectrum of **3a-CD$_3$** can be used to estimate the ν-(C≡N) fundamental as 1898 cm^{-1}. The observed frequency of the ν(C≡N) band is nearly twice the ν(N−CH$_3$) fundamental reported for free methyl isocyanide ($\nu_{N-C} = 945$ cm^{-1}).[21] The

(52) Kubiak, C. P.; Ratliff, K. S. *Isr. J. Chem.* **1991**, *31*, 3.
(53) Bedard, R. L.; Dahl, L. F. *J. Am. Chem. Soc.* **1986**, *108*, 5933.
(54) Rashidi, M.; Kristof, E.; Vittal, J.; Puddephatt, R. J. *Inorg. Chem.* **1994**, *33*, 1497.

(55) Drago, R. S. *Physical Methods in Chemistry*; Saunders College: Orlando, 1977; p 350.
(56) Steel, D. *Theory of Vibrational Spectroscopy*; Saunders: London, 1971; pp 124.
(57) Ebsworth, E. A. V.; Rankin, D. W. H.; Cradock, S. *Structural Methods in Inorganic Chemistry*; Blackwell Scientific: Oxford, 1987; Chapter 5.
(58) Cotton, F. A. *Chemical Applications of Group Theory*; Wiley: New York, 1990; Chapter 10.
(59) Overend, J. In *Infrared Spectroscopy and Molecular Structure*; Davies, M., Ed.; Elsevier: London, 1963; Chapter 10.

Table 8. FT-IR Data for Isotopically Labeled (Methyl Isocyanide Only) $[Ni_3(\mu_3\text{-CNCH}_3)(\mu_3\text{-I})(\mu_2\text{-dppm})_3]^+$ Clusters

compd	isocyanide cap	$\nu(C\equiv N),^a\ cm^{-1}$
3a	$CNCH_3$	1927, 1872
3a-^{13}C	$^{13}CNCH_3$	1891, 1829
3a-^{15}N	$C^{15}NCH_3$	1894, 1833
3a-$^{13}CH_3$	$CN^{13}CH_3$	1905, 1832
3a-CD_3	$CNCD_3$	1898

^{a} Recorded as KBr pellets.

Table 9. Fermi Resonance Eigenvalues for $[Ni_3(\mu_3\text{-CNCH}_3)(\mu_3\text{-I})(\mu_2\text{-dppm})_3]^+$ (**3a**)

band (cm^{-1})	**3a**		free	
	obsd^a	calcd^b	CNCH$_3^c$	CNCD$_3^c$
$\nu(C\equiv N)$	1898	1901	2166	2165
$\nu(N-C)$		939	945	877
$2\nu(N-C)$		1878	1890	1750
W		10		

^{a} Taken from the IR spectrum of **3a-CD₃**, recorded as a KBr pellet. ^{b} Best fit for eigenvalues of eq 4 for all isotopes except **3a-CD₃** and assuming otherwise harmonic isotopic shifts. ^{c} Free methyl isocyanide in the gas phase, see: Mottern, J. G.; Fletcher, W. H. *Spectrochim. Acta* **1962**, *18*, 995.

two $\nu(C\equiv N)$ bands observed in **3a** are interpreted as arising from Fermi resonance involving the $\nu(C\equiv N)$ fundamental and the first overtone of the $\nu(N-C)$ band. Notably, in the IR spectrum of free CNCH₃, the N−C (single bond) fundamental band was observed to move from 945 to 877 cm^{-1} upon deuterium labeling, a change of 68 cm^{-1}.[21] The substitution of CD₃ for CH₃ in **3a-CD₃** lowers the frequency of the $\nu(N-C)$ fundamental sufficiently that the conditions for Fermi resonance are no longer satisfied. Hence, only one $\nu(C\equiv N)$ band is observed for **3a-CD₃**. Significantly, two bands are only observed with the isocyanide-capped and not the carbonyl-capped clusters, lending credence to the idea that Fermi resonance arises from the interaction of the C≡N triple bond and the N−C single bond of the isocyanide (C≡N−C(alkyl)). Fermi resonance perturbed frequencies can be calculated in terms of the unperturbed frequencies $\nu(C\equiv N)$, $2\nu(N-CH_3)$, and the interaction energies $W_{\nu',2\nu''}$ using the secular determinant in eq 4.[58]

$$\begin{vmatrix} 2\nu(N-CH_3) - \nu''_{obs} & W_{\nu',2\nu''} \\ W_{\nu',2\nu''} & \nu(C\equiv N) - \nu'_{obs} \end{vmatrix} = 0 \qquad (4)$$

A best fit of the IR spectra of **3a**, **3a-^{13}C**, **3a-^{15}N**, and **3a-^{13}CH₃** give values of $\nu(C\equiv N)$ = 1901 cm^{-1} and $\nu(N-C)$ = 939 cm^{-1}. These results are collected in Table 9. Our calculations using the various isotopomers are consistent with the observed unperturbed $\nu(C\equiv N)$ band in **3a-CD₃** and the reported value for $\nu(N-C)$ in free methyl isocyanide; the $\nu(N-C)$ band in **3a** could not be definitively assigned. In conclusion, the appearance of two $\nu(C\equiv N)$ bands for this class of isocyanide-capped clusters is due to a Fermi resonance involving the $\nu(C\equiv N)$ fundamental and the first overtone of the $\nu(N-C)$ fundamental. While this is the first report of Fermi resonance in μ_3-η^1 bound isocyanides, our results indicate that the IR spectra of other clusters containing an isocyanide ligand coordinated in a linear

manner, with a $\nu(C\equiv N)$ fundamental near 1900 cm^{-1}, should also exhibit two $\nu(C\equiv N)$ bands.

Summary. The dihalide-capped clusters $Ni_3(\mu_3\text{-X})_2(\mu_2\text{-dppm})_3$ (X = I (**1a**), Br (**1b**)) were synthesized and converted to their respective monocations **1a**$^+$ and **1b**$^+$. Complexes **1a** and **1a**$^+$ were also characterized by X-ray crystallography. Clusters **1a** and **1b** were used in ligand-substitution reactions to conveniently generate a series of isocyanide-capped clusters (**3**−**17**). Several of the isocyanide- and iodo-capped clusters are known electrocatalysts for the reduction of carbon dioxide. In addition, carbon monoxide is able to displace the iodide ligand in **1a** to generate the carbonyl-capped cluster **2a**. Cluster **2a** was also characterized by X-ray crystallography. The carbonyl- and isocyanide-capped clusters **2**−**17** have similar physical and spectroscopic properties. The electrochemical properties are also similar as clusters **2**−**17** all undergo a reversible single-electron reduction at *ca.* −1.1 V *vs* SCE. A molecular orbital study indicates that the LUMO of **2**−**17** is largely metal based. It is the insensitivity of the LUMO to the capping π-acceptor ligands that is responsible for the narrow range of reduction potentials measured for **2**−**17**. The molecular orbital study was also the key to understanding the electronic differences between the dihalide- (**1**) and isocyanide-capped (**3**−**17**) clusters. An unprecedented characteristic of the isocyanide-capped clusters **3**−**17** is that IR spectra show two $\nu(C\equiv N)$ bands both in the solid state and in solution. Isotope labeling studies demonstrated that the appearance of two $\nu(C\equiv N)$ bands for this class of isocyanide-capped clusters is due to a Fermi resonance involving the $\nu(C\equiv N)$ fundamental and the first overtone of the $\nu(N-C(alkyl))$ fundamental. The Fermi resonance is caused by the unique symmetry and energetics of μ_3-η^1 isocyanides. The phenomenological basis for the Fermi resonance is a $\nu(C\equiv N)$ fundamental frequency of *ca.* 1900 cm^{-1}, close in energy to the $\nu(N-C(alkyl))$ overtone, *ca.* 2 (945 cm^{-1}). In the μ_3-η^1 geometry these modes will always possess the same symmetry.

Supporting Information Available: Tables of crystal data and structure refinement, atomic coordinates, positional and anisotropic thermal parameters, bond distances and angles, and derived hydrogen atom coordinates and isotropic thermal parameters for **1a**, **1a**$^+$, and **2a** (101 pages); listing of observed and calculated structure factor tables for **1a**, **1a**$^+$, and **2a** (63 pages). This material is contained in many libraries on microfiche, immediately follows this article in the microfilm version of the journal, can be ordered from the ACS, and can be downloaded from the Internet; see any current masthead page for ordering information and Internet instructions.